

Multipartite quantum correlated bright frequency combs

A. Bensemhoun¹, S. Cassina², C. Gonzalez-Arciniegas³, M. F. Melalkia^{1*}, G. Patera⁴, J. Faugier-Tovar⁵, Q. Wilmart⁵, S. Olivier⁵, A. Zavatta⁶, A. Martin¹, J. Etesse¹, L. Labonté¹, O. Pfister³, V. D'Auria^{1†}, and S. Tanzilli¹

¹*Université Côte d'Azur, CNRS, Institut de Physique de Nice, 17 rue Julien Lauprêtre, 06200 Nice, France.*

²*University of Insubria, Department of Science and High Technology, via Valleggio 11, 22100 Como, Italy*

³*University of Virginia Physics Department, 382 McCormick Rd, Charlottesville, VA 22903, USA.*

⁴*University of Lille, CNRS, UMR 8523 – PhLAM – Physique des Lasers Atomes et Molécules, F-59000 Lille, France.*

⁵*CEA-LETI, Université Grenoble Alpes, F-38000 Grenoble, France and*

⁶*Istituto Nazionale di Ottica (CNR-INO), CNR, Largo Enrico Fermi 6, 50125 Firenze, Italy*

This experimental work demonstrates multipartite quantum correlation in bright frequency combs out of a microresonator integrated on silicon nitride working above its oscillation threshold. Multipartite features, going beyond so far reported two-mode correlation, naturally arise due to a cascade of non-linear optical processes, making a single-color laser pump sufficient to initiate their generation. Our results show the transition from two-mode to multipartite correlation, witnessed by noise reductions as low as -2.5 dB and -2 dB, respectively, compared to corresponding classical levels. A constant of the movement of the non-linear interaction Hamiltonian is identified and used to assess the multipartite behavior. Reported demonstrations pave the way to next generation on-chip multipartite sources for quantum technologies applications.

PACS numbers:

I. INTRODUCTION

Optical multipartite states that exploit continuous variable (CV) encoding are key resources for quantum information science [1], playing a crucial role in measurement-based optical quantum computing [2, 3], multipartner secure quantum networks [4] and quantum metrology [5]. Future, ambitious applications require multipartite quantum systems to combine the ability to generate and manipulate entanglement over a high number of modes with devices' robustness and small footprints. A prominent solution to scale up the size of multipartite states is offered by CV entanglement between optical modes at different frequencies; this choice allows working with large numbers of correlated subsystems [6–8] that, if required, can be easily separated as functions of their colors [1]. In parallel, integrated photonics on silicon (Si) and silicon nitride (SiN) has become a go-to solution to reduce the physical size of optical systems while benefitting from the advantages of cascaded optical components on CMOS compatible platforms [9–11].

In this context, frequency combs generated by non-linear interactions in silicon-based microresonators (microcombs) bridge advantageously multipartite entanglement and integrated resources [11]. Si and SiN microrings and disks are identified as natural room-temperature sources of CV frequency/time entanglement via four wave mixing (FWM). Their quantum dynamics has been the object of multiple theoretical works [12–15], while experimental demonstrations have proven these

devices able to generate two-color CV correlation in paired modes in both below [16–19] and above threshold regimes [20–22]. A signature of multimode features has been measured from second order photon correlation in solitons out of devices far above threshold [23].

This paper goes beyond two-color analysis to demonstrate experimentally that multipartite behavior is naturally present in bright microcombs from above-threshold SiN-microrings. CV multipartite dynamics is explored here by measuring quantum intensity correlation between up to four bright optical modes generated by an SiN microring. The analysis of intensity correlation makes it possible to observe that, when driving the system progressively farther above threshold, a transition takes place from a bipartite regime to a multipartite one at four modes and beyond. Remarkably, the generation of the multipartite state is initiated by a single monochromatic pump at the input of the device as was predicted in a previous theoretical work [24]. These results pave the way to a new operation regime for quantum microcombs and have a double impact. Conceptually, they push silicon-based microresonators beyond one-to-one correlation reported so far [16–22], therefore exploring their potential for high-dimensional state connectivity and its applications in quantum photonics. From the practical point of view, they show that multipartite frequency correlation can be obtained by releasing the condition of multi-color pumps at the input of non-linear sources, unlike previous CV experiments [6–8].

*Present address: Laboratoire Systèmes Lasers, Ecole Militaire Polytechnique, BP 17 Bordj El Bahri, 16046 Algiers, Algeria

†Contact author: virginia.dauria@univ-cotedazur.fr

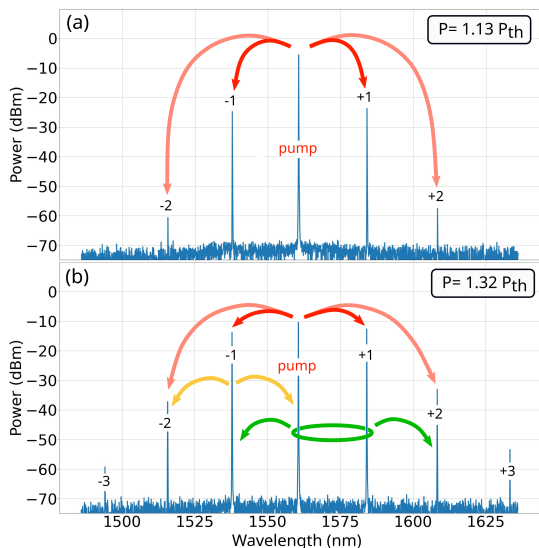


FIG. 1: Measured optical spectra of the comb generated by the SiN microring operating above the oscillation threshold for input pump powers of (a) $P = 1.13 P_{th}$ and (b) $P = 1.32 P_{th}$, where P_{th} is the pump corresponding to the threshold. The figure shows some of the multiple non-linear processes that can simultaneously take place, including degenerate FWM of the input pump (red) or of a secondary mode (yellow), as well as non-degenerate FWM of two of the comb modes (green). Self- and cross-phase modulations are not shown to preserve the drawing legibility.

II. MULTIPARTITE CORRELATION IN BRIGHT MICROCOMBS

A. Concepts and experimental setup

In above threshold FWM, the generation of bright frequency combs is associated with rich dynamics [9, 14, 25, 26]. Figure 1 shows some examples of primary microcombs out of the SiN microring, measured by an optical spectrum analyzer (OSA). The system is pumped with a continuous wave (CW) input laser and operates at moderate distance from the threshold, well below the soliton regime [25]; as shown in the figure, bright modes, including the input pump, are all in the telecom c-band. In these conditions, different FWM processes can take place [24]. The single CW laser generates via degenerate FWM a primary comb of paired modes, symmetrically distributed with respect to the pump line (see modes ± 1 , ± 2 in Figure 1-a). Such bright components provide, in turn, additional pumps for other degenerate or non-degenerate FWM processes (see Figure 1-b). The coexistence of such simultaneous FWMs makes multipartite physics arise in a natural way when increasing the modes' powers [24]. The higher is the input pump power, P , the more number of modes, as well as their relative power, increase making their contribution to secondary interactions non-negligible anymore.

The experimental setup used to generate and to in-

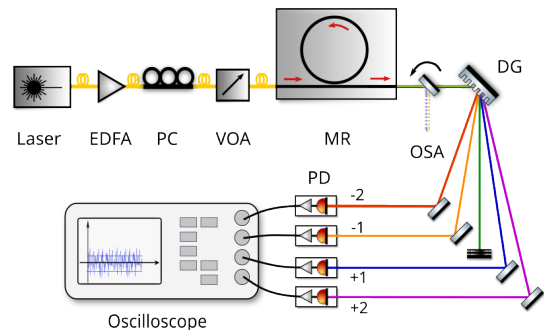


FIG. 2: Experimental setup for the measurement of intensity correlations at the output of an SiN microring (MR) above threshold. Modes ± 1 and ± 2 are separated by a grating (DG) thanks to their different colors and their intensities are individually detected (PD). The corresponding photocurrents are evaluated in the Fourier transform domain and digitally combined as required to evaluate the correlation among different modes. Noise power spectrum of combined signals are used to retrieve non-classical features. Noise are evaluated with respect to shot noise signals obtained by sending to the detectors laser beams whose powers match those of the modes under scrutiny.

vestigate the multipartite state is sketched in Figure 2. Before the microring, the setup is entirely made of plug-n-play telecom components based on optical fibers. The master source is a fiber-coupled CW laser (RIO-Orion) delivering 12 mW at 1560.053 nm with a fine tunability of ≈ 40 pm. The laser output is amplified by an Erbium Doped Fiber Amplifier (EDFA), whose working point is optimized to reduce noise contributions. Downstream of the EDFA, two wavelength demultiplexing stages (not represented) are used to reduce amplified spontaneous emission. After an in-line variable optical attenuator (VOA), the laser polarization is adjusted (PC) to match the transverse electric (TE) mode of the microring, whose propagation losses were measured to be the lowest. The laser light is edge-coupled via a microlensed fiber into the microring and used as the input pump of the FWM process. Fiber-to-chip coupling losses are of about -3 dB. The microring is fabricated in-house at the CEA-LETI on Si_3N_4 [27, 28]. It is a single-pass microring (MR, see Figure 2) with a radius of 112 μm (corresponding to a free spectral range of 200 GHz) coupled to a straight waveguide set at a gap of 300 nm. The width and height of all waveguides are, respectively, 1.9 μm and 800 nm. The MR is mounted on a thermo-electric cooler (TEC) that stabilizes its temperature at 68.5°C. The microring has an intrinsic $Q \sim 10^6$ and operates in the overcoupling regime, with a measured pump oscillation threshold $P_{th} = 53 \pm 3$ mW. Its output is collected in free space with a microscope objective. A low-loss diffraction grating splits the comb's optical components and sends them to separate photodiodes (PD). Four modes (± 1 and ± 2) are simultaneously detected. Overall optical losses per mode lead to a detection efficiency of about 70%. To evaluate the intensity

correlation, the PD photocurrents are acquired by a fast oscilloscope to be evaluated in the Fourier domain and digitally combined. Noise power spectra of combined signals are used to retrieve non-classical features. All noise spectra are evaluated with respect to shot noise levels (SNL) that are obtained by sending to the detectors four laser beams whose mean intensities match those of the modes under scrutiny. A flip mirror before the grating is used to send the light to the OSA to check the MR's operation regime before any measurement.

B. Quantifying multipartite intensity correlation

The overall system dynamics is described by the general FWM Hamiltonian, \hat{H}_{FWM} . It contains all processes by which two photons in frequency modes p and q annihilate to create paired photons in modes s and r [13, 24]:

$$\hat{H}_{FWM} = \sum_{rspq} \delta_{r+s,p+q} \hat{a}_r^\dagger \hat{a}_s^\dagger \hat{a}_p \hat{a}_q, \quad (1)$$

where \hat{a}_i and \hat{a}_i^\dagger are the bosonic operators associated to intracavity modes $i = 0, \pm 1, \pm 2, \dots$ and satisfy $[\hat{a}_i, \hat{a}_j^\dagger] = \delta_{i,j}$ and $[\hat{a}_i, \hat{a}_j] = 0$. The sum over all modes describes the fact that, above threshold, any pair of frequency modes can play the role of pumps for another FWM process, provided the energy conservation, expressed by the Kronecker delta, is respected (*i.e.* $\omega_r + \omega_s = \omega_p + \omega_q$, where ω is the mode optical frequency). Cross- and self-phase correlation terms are included in \hat{H}_{FWM} [24]. The non-linear interaction coupling constant is set to 1 for simplicity.

Given $2M + 1$ interacting modes, it is easy to prove that the Hamiltonian of Eq. (1) admits as a constant of motion the observable associated with the Hermitian operator:

$$\hat{C} = \sum_{k=-M}^{+M} k \hat{n}_k = \hat{n}_1 - \hat{n}_{-1} + 2(\hat{n}_2 - \hat{n}_{-2}) + \dots, \quad (2)$$

with $\hat{n}_k = \hat{a}_k^\dagger \hat{a}_k$ and $k \in \mathbb{N}$. The operator \hat{C} commutes with the time independent Hamiltonian \hat{H}_{FWM} , meaning that the associated physical quantity is conserved throughout the system evolution. In the case of a non-seeded microresonator, apart from the input pump ($k = 0$), all modes $\pm k$ are initially in the vacuum state, leading to both $\langle \hat{C} \rangle$ and $\text{Var}(\hat{C}) = \langle \hat{C}^2 \rangle - \langle \hat{C} \rangle^2$ equal to 0. These values are expected to remain constant even after the FWM interaction, when the modes are populated by bright beams. In particular, the variance of \hat{C} contains both quantum noise associated with individual modes and covariance terms describing intermodal quan-

tum correlation. It can be written as:

$$\begin{aligned} \text{Var}(\hat{C}) &= \sum_{k=0}^{+M} k^2 \text{Var}(\hat{n}_k - \hat{n}_{-k}) \\ &+ \sum_{\substack{k,l=0 \\ k \neq l}}^{+M} k l \text{Cov}(\hat{n}_k - \hat{n}_{-k}, \hat{n}_l - \hat{n}_{-l}), \end{aligned} \quad (3)$$

where $\text{Cov}(\hat{O}, \hat{O}') = \langle \hat{O} \hat{O}' \rangle - \langle \hat{O} \rangle \langle \hat{O}' \rangle$. Covariance terms in Equation (3) are in general non-negligible for multipartite systems. In the following, a $\text{Var}(\hat{C})$ below the shot noise level is used to witness quantum intensity correlation involving all interacting modes. This choice allows introducing a measure of multipartite correlation in intensity, differing from other common correlation witnesses that are based on field quadratures [1]. Also note that \hat{C} represents one of the symmetries of the FWM Hamiltonian. Its associated evolution operator, $\mathcal{U}(\theta) = \prod_{k=-M}^M e^{i\theta k \hat{n}_k}$, is the operator that simultaneously phase shifts all modes k , each by an angle $k\theta$. H is invariant under $\mathcal{U}(\theta)$, $\forall \theta$.

III. RESULTS

In experiments, \hat{C} can directly be measured by simultaneously acquiring the intensities of all involved modes, $I_i \propto \hat{n}_i$, as functions of time. Figure 3 shows intensity correlation between modes ± 1 (a-blue), modes ± 2 (a-red) and the variance of \hat{C} on the ensemble of the four modes (b). Curves are plotted as functions of the input pump power, P , normalized to P_{th} . Bimodal intensity correlation are expressed in terms of the noise on their intensity difference that is proportional to $\text{Var}(\hat{n}_k - \hat{n}_{-k})$. This approach has been already adopted to study modes ± 1 in bright microcombs [20, 21].

At low pump powers, the leading non-linear process is the degenerate FWM of the input laser beam that produces symmetric modes (see Figure 1-a). This leads to one-to-one correlation between modes ± 1 , that are, to first approximation, independent of ± 2 . This regime corresponds to the optimal intensity correlation of -2.5 dB at low P/P_{th} plotted in Figure 3-a. When increasing P , the intensity correlation of modes ± 1 is degraded, eventually reaching ≈ -1 dB. Such a change can be associated with the appearance of cascaded FWM processes that link the dynamics of ± 1 to that of ± 2 , and then to that of ± 3 , and so on to higher-order modes [24]. Under these conditions, multipartite correlation arise and detecting only two modes corresponds to tracing out a part of the multipartite system; the measurement of $\text{Var}(\hat{n}_1 - \hat{n}_{-1})$ thus becomes insufficient to fully characterize intensity correlation available at the microring output. This behavior is qualitatively reproduced by correlation between modes ± 2 , never observed so far in experiments [20, 22]. Lesser

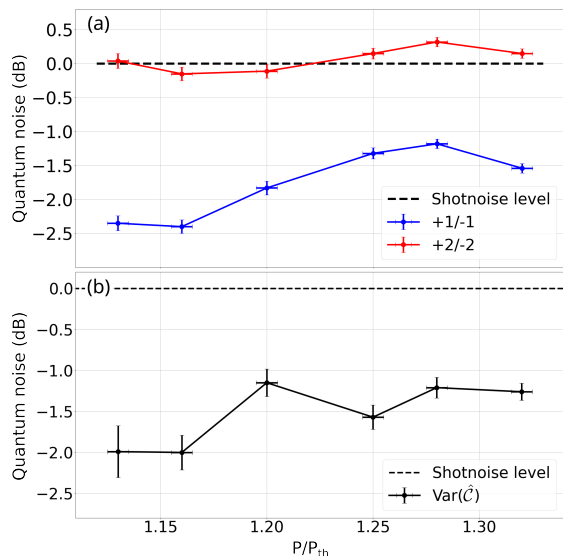


FIG. 3: (a) Quantum correlation normalized to the shotnoise level as a function of the input pump power between +1/-1 (blue) and +2/-2 (red). (b) Quantum noise normalized on the shotnoise level of the multipartite observable as a function of the input pump power. Experimental data are not corrected by quantum efficiency, only for residual electronic noise. All values refer to noise level evaluated at the same analysis frequency ($\approx 4\text{MHz}$). For each of the curves the shot noise has been experimentally obtained by replacing each of the beams under scrutiny with a coherent beam of the same mean power

noise reductions in such modes are due to reduced signal-to-noise ratio when measuring weak intensity signals.

The measurement of \hat{C} combines these results for the ensemble of the 4 modes. As expected, $\text{Var}(\hat{C}) < \text{SNL}$ for all considered input pump powers, going down to -2 dB at low P . Remarkably, this stays true despite the fact that, for this microcomb, $\text{Var}(\hat{n}_2 - \hat{n}_{-2})$ stays high and, eventually, passes above its SNL. Evidence of a four-partite correlation is even stronger when comparing experimental results on $\text{Var}(\hat{C})$ with $\text{Var}(\hat{C}_{\text{NC}}) = \sum_k k^2 \text{Var}(\hat{n}_k - \hat{n}_{-k})$, representing the noise levels that would be obtained on \hat{C} in the absence of covariance terms (see Eq. (3)). $\text{Var}(\hat{C}_{\text{NC}})$ can be estimated, from data on ± 1 and ± 2 , to vary with P/P_{th} from $\approx -1.6\text{dB}$ to $\approx +1\text{dB}$: measured $\text{Var}(\hat{C})$ systematically below these levels confirm the presence of non negligible covariance terms that mitigate residual quantum noise in $\text{Var}(\hat{n}_1 - \hat{n}_{-1})$ and $\text{Var}(\hat{n}_2 - \hat{n}_{-2})$ in Eq. (3). For the microcomb of Figure 3-b, an abrupt decrease of $\text{Var}(\hat{C})$ can be observed at $P/P_{th} \geq 1.20$. Correspondingly, modes ± 3 start being non negligible in the microcombs. Although weaker than modes ± 1 (typically -40 dB), ± 3 terms act as seeds to secondary FWM processes, thus connecting their dynamics to that of other modes. In this regard, note that the measurement of \hat{C} with $M=4$ neglects contributions from symmetric modes ± 3 and higher; the increase of $\text{Var}(\hat{C})$ with P/P_{th} thus gives an indirect proof of a richer dynamics where more than 4 modes are quantum corre-

lated.

To dig into the four-mode regime, a second set of measurements is performed at lower pump values, in a regime where modes ± 3 are expected to be negligible. Note that the microcomb under study in the low power regime is not the same as for measurements in Figure 3. This is due to optical bistability in resonant FWM processes, *i.e.*, to the existence of two stable stationary solutions in above-threshold microresonators [26]; depending on the chosen range of input powers, the system spontaneously emits one microcomb or the other. Figures 4-a) and b) show intensity correlation as functions of low P/P_{th} for symmetric modes; the behavior of $\text{Var}(\hat{n}_k - \hat{n}_{-k})$ qualitatively confirms what has already been observed for the microcomb of Figure 3. Lower measured correlation levels are due to the microcomb emission that is not bright enough to make residual electronics noise negligible. Figures 4-c) and -d) illustrate the dynamics of cross correlation between non-symmetric modes in terms of $\text{Var}(\hat{n}_i - \hat{n}_j)$, with $i \neq j = \pm 1, \pm 2$. At very low powers, secondary FWM processes are not yet well established and quantum correlation only take place between symmetric modes generated by degenerate FWM of the input pump (Figure 4-a) and -b). The reduction of $\text{Var}(\hat{n}_i - \hat{n}_j)$ observed when increasing P bears witness to the birth of multipartite correlation: the links between modes initially independent lead to noises below the classical level at intermediate values of P (4-c) and -d)). The differences between curves of Figure c) and d) can be justified by optical losses and dispersion that can induce same asymmetry on modes +2 and -2. This regime can be considered as showing four-partite features. At $P/P_{th} \approx 1.15$, the growth of modes ± 3 reduces cross-as well as symmetric-mode correlation; this represents a confirmation of a 6-partite dynamics for which neglecting information of modes above ± 2 corresponds to tracing out a part of a larger quantum correlated system. As a final remark, note that the behavior of symmetric and cross mode correlation is well summarized by the $\text{Var}(\hat{C})$ evolution reported in the figure inset. Its steep change at higher power reproduces that of cross correlation and leads to values above the SNL at high powers. For this microcomb, in addition to the appearance of modes ± 3 , it is pertinent to note that the higher is P , the more probable becomes the transition towards the comb corresponding to higher power, thus potentially affecting the system quantum correlation.

IV. CONCLUSION

The presented experimental work demonstrates multipartite features in frequency combs out of an SiN microring exploited above its oscillation threshold. Compared to previously studied systems, multipartite features appear spontaneously due to a cascade of secondary FWM processes that exploit the primary comb out of a degenerate FWM of a monochromatic pump laser. The dy-

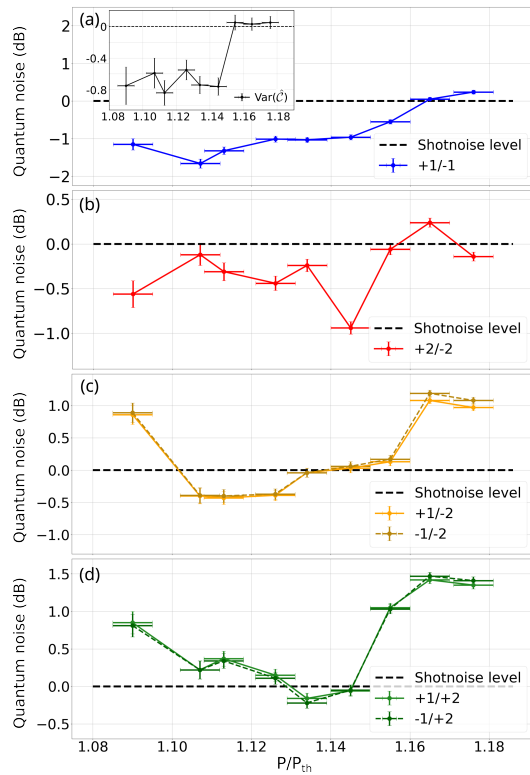


FIG. 4: Quantum correlation normalized to SNL as functions of the input pump power for modes +1/-1 (a), +2/-2 (b) and between non-symmetric modes (c) and (d). The inset reports the corresponding $\text{Var}(\hat{C})$.

namics of quantum correlation in four bright modes is investigated by measuring their one-to-one correlation as well as in terms of the noise of the operator \hat{C} that represents a symmetry of the FWM Hamiltonian and that combines all modes. Although experimental data refer to the first four modes appearing in the primary combs, all obtained results indicate that higher order connectivity can be expected when including in the analysis subsequent components that appear when working farther away from the threshold. Experimental evidence of multipartite correlation in bright microcombs and the study of their dynamics have never been performed before. Pre-

sented results, as well as the theoretical and experimental tools dedicated to their measurement, open the way to the exploitation of microcombs for future quantum technology applications in CV multipartite quantum photonics, with a simple experimental configuration, where just one external CW pump laser is needed to feed the system.

Acknowledgment

This work has been conducted within the framework of the project OPTIMAL granted by the European Union by means of the Fond Européen de développement régional (FEDER). The authors also acknowledge financial support from the Agence Nationale de la Recherche (ANR) through the projects SPHIFA (ANR-20-CE47-0012) and OQulus (ANR-22-PETQ-0013) and from Academy RISE of Université Côte d'Azur. VDA thanks the Institut Universitaire de France for the support. OP acknowledges support from CNRS, Fondation Doebelin, and US NSF grants ECCS-2219760 and PHY-2112867.

Competing interests

The authors declare no competing interests.

Authors' contributions

A.B. mounted the entire experimental setup and took care of data acquisition and analysis, with the help of S.C., M.F.M., and A.Z.; C.G.-A. found the original theoretical tool for witnessing multipartite intensity correlation, with the help of O.P.; S.O. and Q.W. designed and fabricated the SiN integrated structures; V.D'A. and O.P. conducted the data analysis and interpretation, with the help of A.M., J.E., G.P., L.L., and S.T. All authors read, discussed, and contributed to the writing, reviewing, and editing of the manuscript. V.D'A., L.L., and S.T. coordinated and managed the project, ensuring its successful completion.

-
- [1] C. Fabre and N. Treps, *Rev. Mod. Phys.* **92**, 035005 (2020), URL <https://link.aps.org/doi/10.1103/RevModPhys.92.035005>.
- [2] O. Pfister, *Journal of Physics B: Atomic, Molecular and Optical Physics* **53**, 012001 (2020), URL <https://doi.org/10.1088/1361-6455/ab526f>.
- [3] W. Asavanant and A. Furusawa, *Optical Quantum Computers: A Route to Practical Continuous Variable Quantum Information Processing* (AIPP Books, 2022).
- [4] M. Epping, H. Kampermann, C. macchiavello, and D. Bruß, *New Journal of Physics* **19**, 093012 (2017), ISSN 1367-2630, URL <http://dx.doi.org/10.1088/1367-2630/aa8487>.
- [5] X. Guo, C. R. Breum, J. Borregaard, S. Izumi, M. V. Larsen, T. Gehring, M. Christandl, J. S. Neergaard-Nielsen, and U. L. Andersen, *Nature Physics* **16**, 281–284 (2019), ISSN 1745-2481, URL <http://dx.doi.org/10.1038/s41567-019-0743-x>.
- [6] J. Roslund, R. M. De Araujo, S. Jiang, C. Fabre, and N. Treps, *Nature Photonics* **8**, 109 (2014).
- [7] M. Chen, N. C. Menicucci, and O. Pfister, *Physical review letters* **112**, 120505 (2014).
- [8] F. A. S. Barbosa, A. S. Coelho, L. F. Muñoz-Martínez, L. Ortiz-Gutiérrez, A. S. Villar, P. Nussenzveig, and

- M. Martinelli, Physical review letters **121**, 073601 (2018).
- [9] Y. K. Chembo, E. Heidari, and C. R. Menyuk, Applied Physics Letters **123** (2023), ISSN 1077-3118, URL <http://dx.doi.org/10.1063/5.0181707>.
- [10] L. S. Madsen, F. Laudenbach, M. F. Askarani, F. Rortais, T. Vincent, J. F. F. Bulmer, F. M. Miatto, L. Neuhaus, L. G. Helt, M. J. Collins, et al., Nature **606**, 75–81 (2022), ISSN 1476-4687, URL <http://dx.doi.org/10.1038/s41586-022-04725-x>.
- [11] L. Labonté, O. Alibart, V. D’Auria, F. Dautre, J. Etesse, G. Sauder, A. Martin, E. Picholle, and S. Tanzilli, PRX Quantum **5**, 010101 (2024), URL <https://link.aps.org/doi/10.1103/PRXQuantum.5.010101>.
- [12] Y. K. Chembo and N. Yu, Phys. Rev. A **82**, 033801 (2010), URL <https://link.aps.org/doi/10.1103/PhysRevA.82.033801>.
- [13] E. Gouzien, L. Labonté, J. Etesse, A. Zavatta, S. Tanzilli, V. D’Auria, and G. Patera, Phys. Rev. Res. **5**, 023178 (2023), URL <https://link.aps.org/doi/10.1103/PhysRevResearch.5.023178>.
- [14] M. A. Guidry, D. M. Lukin, K. Y. Yang, and J. Vučković, Optica **10**, 694 (2023), ISSN 2334-2536, URL <http://dx.doi.org/10.1364/OPTICA.485996>.
- [15] M. Sloan, A. Viola, M. Liscidini, and J. E. Sipe (2024), 2409.10639, URL <https://arxiv.org/abs/2409.10639>.
- [16] V. D. Vaidya, B. Morrison, L. Helt, R. Shahrokshahi, D. Mahler, M. Collins, K. Tan, J. Lavoie, A. Reppingon, M. Menotti, et al., Science advances **6**, eaba9186 (2020).
- [17] Y. Zhang, M. Menotti, K. Tan, V. Vaidya, D. Mahler, L. Helt, L. Zatti, M. Liscidini, B. Morrison, and Z. Vernon, Nature communications **12**, 2233 (2021).
- [18] Z. Yang, M. Jahanbozorgi, D. Jeong, S. Sun, O. Pfister, H. Lee, and X. Yi, Nature Communications **12**, 4781 (2021).
- [19] M. Jahanbozorgi, Z. Yang, S. Sun, H. Chen, R. Liu, B. Wang, and X. Yi, Optica **10**, 1100 (2023).
- [20] A. Dutt, K. Luke, S. Manipatruni, A. L. Gaeta, P. Nussenzveig, and M. Lipson, Physical Review Applied **3**, 044005 (2015).
- [21] Y. Shen, P.-Y. Hsieh, S. K. Sridhar, S. Feldman, Y.-C. Chang, T. A. Smith, and A. Dutt, *Strong nanophotonic quantum squeezing exceeding 3.5 db in a foundry-compatible kerr microresonator* (2024), 2411.11679, URL <https://arxiv.org/abs/2411.11679>.
- [22] R. Alfredo Kö*gler, G. Couto Rickli, R. Ribeiro Domenegueti, X. Ji, A. L. Gaeta, M. Lipson, M. Martinelli, and P. Nussenzveig, Optics Letters **49**, 3150 (2024).
- [23] M. A. Guidry, D. M. Lukin, K. Y. Yang, R. Trivedi, and J. Vučković, Nature Photonics **16**, 52 (2022).
- [24] A. Bensemhoun, C. Gonzalez-Arciniegas, O. Pfister, L. Labonté, J. Etesse, A. Martin, S. Tanzilli, G. Patera, and V. d’Auria, Physics Letters A **493**, 129272 (2024).
- [25] M. Karpov, M. H. Pfeiffer, H. Guo, W. Weng, J. Liu, and T. J. Kippenberg, Nature Physics **15**, 1071 (2019).
- [26] C. Godey, I. V. Balakireva, A. Coillet, and Y. K. Chembo, Phys. Rev. A **89**, 063814 (2014), URL <https://link.aps.org/doi/10.1103/PhysRevA.89.063814>.
- [27] H. E. Dirani, L. Youssef, C. Petit-Etienne, S. Kerdiles, P. Grosse, C. Monat, E. Pargon, and C. Sciancalepore, Opt. Express **27**, 30726 (2019), URL <https://opg.optica.org/oe/abstract.cfm?URI=oe-27-21-30726>.
- [28] Q. Wilmart, S. Guerber, J. Faugier-Tovar, Y. Ibrahimi, C. Petit-Etienne, L. Youssef, C. Socquet-Clerc, A. Myko, K. Ribaud, F. Duport, et al., in *Silicon Photonics XVII*, edited by G. T. Reed and A. P. Knights, International Society for Optics and Photonics (SPIE, 2022), vol. 12006, p. 120060D, URL <https://doi.org/10.1117/12.2606853>.